



HAL
open science

Saturating light induces sustained accumulation of oil in plastidal lipid droplets in *Chlamydomonas reinhardtii*

Hugh Douglas Goold, Stéphan Cuiné, Bertrand Legeret, Yuanxue Liang, Sabine Brugière, Pascaline Auroy, Hélène Javot, Marianne Tardif, Brian Jones, Fred Beisson, et al.

► To cite this version:

Hugh Douglas Goold, Stéphan Cuiné, Bertrand Legeret, Yuanxue Liang, Sabine Brugière, et al. Saturating light induces sustained accumulation of oil in plastidal lipid droplets in *Chlamydomonas reinhardtii*. *Plant Physiology*, 2016, 171 (4), pp.2406-2417. 10.1104/pp.16.00718 . hal-02065372

HAL Id: hal-02065372

<https://hal.science/hal-02065372v1>

Submitted on 4 Sep 2024

HAL is a multi-disciplinary open access archive for the deposit and dissemination of scientific research documents, whether they are published or not. The documents may come from teaching and research institutions in France or abroad, or from public or private research centers.

L'archive ouverte pluridisciplinaire **HAL**, est destinée au dépôt et à la diffusion de documents scientifiques de niveau recherche, publiés ou non, émanant des établissements d'enseignement et de recherche français ou étrangers, des laboratoires publics ou privés.

1 **Research Area:** Biochemistry and Metabolism (Plant Physiology)

2 **Short title:** High light induces reserve accumulation in *Chlamydomonas*

3

4 *Corresponding to: Yonghua Li-Beisson (yonghua.li@cea.fr)

5 CEA Cadarache, France Tel: +33 4 42 25 28 97 Fax: +33 4 42 25 62 65

6

7 **Saturating Light Induces Sustained Accumulation of Oil Primarily Stored in Lipid**
8 **Droplets of Plastidial Origin in *Chlamydomonas reinhardtii***

9

10 Hugh Douglas Goold^{1,2}, Stéphan Cuiné¹, Bertrand Légeret¹, Yuanxue Liang¹, Sabine
11 Brugière³, Pascaline Auroy¹, Hélène Javot¹, Marianne Tardif³, Brian Jones², Fred Beisson¹,
12 Gilles Peltier¹, Yonghua Li-Beisson^{1*}

13

14 ¹CEA, CNRS, Aix Marseille Université, UMR7265, Institut de Biosciences et
15 Biotechnologies, Cadarache, 13108, France

16 ²Faculty of Agriculture and the Environment, University of Sydney, Australia

17 ³CEA, INSERM, Université Grenoble Alpes, Institut de Biosciences et Biotechnologies de
18 Grenoble, U1038, Grenoble, 38000, France

19

20 **One sentence summary**

21 Saturating light induces oil storage in *Chlamydomonas*, and the newly formed oil accumulate
22 in lipid droplets distinct in protein and lipid compositions from those induced by nitrogen
23 starvation.

24

25 **AUTHOR CONTRIBUTIONS**

26 H.G., G.P., B.J., F.B., Y. L-B designed research; H.G., S.C., B.L., Y.L., H.J., S.B., P.A.
27 performed research; H.G., M.T., B. L., Y.L., H.J., M.T., F.B., G.P., Y. L-B analysed data;
28 H.G., F.B., M.T., G.P., Y. L-B wrote the paper. All authors agreed on the manuscript.

29

30

31

32

33

34

35 **ABSTRACT**

36 Enriching algal biomass in energy density is an important goal in algal biotechnology.
37 Nitrogen (N) starvation is considered the most potent trigger of oil accumulation in
38 microalgae and has been thoroughly investigated. However, N-starvation causes slow down
39 and eventually arrest of biomass growth. In this study, we show that exposing a
40 *Chlamydomonas reinhardtii* culture to saturating light (SL) under a non-limiting CO₂
41 concentration in turbidostatic photobioreactors induces a sustained accumulation of lipid
42 droplets (LDs) without compromising growth, which results in much higher oil productivity
43 than N starvation. We also show that the polar membrane lipid fraction of SL-induced LDs
44 are rich in plastidial lipids (~70%), in contrast to N-starvation induced LDs which contain
45 ~60% lipids of ER origin. Proteomic analysis of LDs isolated from SL-exposed cells
46 identified >200 proteins, including known proteins of lipid metabolism, as well as 74 proteins
47 uniquely present in SL-induced LDs. LDs induced by SL and N-depletion thus differ in
48 protein and lipid contents. Taken together, lipidomic and proteomic data thus show that a
49 large part of the sustained oil accumulation occurring under SL is likely due to the formation
50 of plastidial LDs. We discuss our data in relation to the different metabolic routes used by
51 microalgae to accumulate oil reserves depending on cultivation conditions. Finally, we
52 propose a model in which oil accumulation is governed by an imbalance between
53 photosynthesis and growth, which can be achieved by impairing growth or by boosting
54 photosynthetic carbon fixation, with the latter resulting in higher oil productivity.

55

56 **Key Words:** Microalgae, Biomass, High light, Lipidomics, Productivity, Energy imbalance

57

58

59

60

61

62

63

64

65

66

67

68

69 INTRODUCTION

70

71 Neutral lipid accumulation by microalgae has recently regained intensive interest because
72 these organisms are considered promising as a feedstock for the production of renewable
73 fuels and fatty acid (FA)-derivatives (Rosenberg et al., 2008; Wijffels and Barbosa, 2010;
74 Khozin-Goldberg and Cohen, 2011). Most microalgal species do not accumulate large
75 amounts of neutral lipids (i.e. triacylglycerols TAGs) when grown under optimal conditions
76 (Sheehan, 1998). Neutral lipid accumulation can, however, be induced by exposing cells to
77 unfavourable culture conditions, for example: removing nutritional elements (nitrogen,
78 sulphur, iron, phosphate etc) from the media; increasing salinity or growth temperature
79 (Moellering and Benning, 2010; Siaut et al., 2011; Urzica et al., 2013; Abida et al., 2015;
80 Légeret et al., 2016); or exposing cells to small chemically active molecules (Kato et al.,
81 2013; Kim et al., 2013; Kim et al., 2015). Most of the current understanding of TAG
82 metabolism in *C. reinhardtii* has been gained through the study of molecular mechanisms
83 occurring during N starvation response (Fan et al., 2011; Goodson et al., 2011; Siaut et al.,
84 2011; Tsai et al., 2014; Tsai et al., 2015). It is uncertain if the mechanisms of TAG
85 accumulation upon N starvation are generally applicable or whether different mechanisms are
86 employed under other types of conditions. A major limitation in the use of microalgae to
87 produce oil is the fact that nitrogen (N) deprivation, as well as most other TAG-inducing
88 conditions, provoke impairment in protein synthesis and cell division, thus limiting
89 productivity (Hu et al., 2008; Scott et al., 2010).

90 Biomass productivity is the result of highly co-ordinated cellular processes starting
91 with the capture of light by photosystems, fixation of CO₂ through the Calvin-Benson Cycle,
92 to cell growth and division. Light is one of the most variable environmental parameters
93 during the growth of photoautotrophs in natural environments. In non-saturating light, CO₂
94 fixation and biomass productivity increase linearly as a function of light intensity. Above a
95 certain threshold, light saturation occurs. A considerable body of work has documented the
96 effects of high light on photosynthesis, including the effects on the pigment content (Bonente
97 et al., 2012), on the induction of dissipation or protection mechanisms (Peers et al., 2009),
98 and on the production of reactive oxygen species (ROS) (Fischer et al., 2006; Forster et al.,
99 2006; Erickson et al., 2015; Sato et al., 2015). The effect of light intensity on carbon
100 allocation and reserve formation has also been explored (Pal et al., 2011; Fan et al., 2012;
101 Klok et al., 2013; He et al., 2015). For example, increasing light intensity has been shown to
102 increase the cellular neutral lipid content in a number of microalgal species, including

103 *Haematococcus pluvialis* (Zhekisheva et al., 2002), *Tichocarpus crinitus* (Khotimchenko and
104 Yakovleva, 2005) and in *Chlamydomonas reinhardtii* (Mettler et al., 2014). Molecular factors
105 involved in TAG storage under high light are still to be uncovered.

106 Oil accumulation is associated with the formation of lipophilic droplets, called lipid
107 droplet (LDs) (or oil bodies, or oleosomes) (Jolivet et al., 2013). LDs are specialized
108 intracellular organelles made of a neutral lipid core surrounded by a membrane lipid coat in
109 which proteins are embedded (Huang, 1996). LDs serve as a temporary storage site for
110 neutral lipids, and also participate in the active synthesis and metabolisms of these non-
111 membrane forming lipids (Goodman, 2008; Farese Jr and Walther, 2009; Chapman et al.,
112 2012; Goold et al., 2014; Tsai et al., 2015). The current model of LD biogenesis suggests that
113 these lipid-rich subcellular structures arise from membrane ‘budding’ or ‘blistering’, thus the
114 lipid molecules present in the LD lipid coat infer its origin of biogenesis. For example, oil
115 bodies in the oilseed are coated by a mono-layer of lipids of mostly ER-origin (Huang, 1992;
116 Tzen and Huang, 1992) whereas plastoglobules are covered by lipids usually found as part of
117 the thylakoid membranes (Austin et al., 2006). Thus, protein and lipid composition of LDs
118 can shed light on the likely subcellular location of TAG synthesis and LD biogenesis.
119 Compared to oilseeds, the unicellular microalga *C. reinhardtii* offers an excellent platform to
120 study LD formation due to the ease with which researchers can induce lipid droplet
121 biogenesis or degradation by simply changing the culture media (Goodson et al., 2011; Goold
122 et al., 2014; Tsai et al., 2015).

123 Here, we have used a turbidostatic continuous cultivation system to study the effect of
124 light intensity on oil accumulation and productivity in *C. reinhardtii* cells. We report that
125 exposure to a saturating light (SL) leads to increased cellular oil content and to much higher
126 oil productivity than observed in response to N-depletion. A general model in which oil
127 accumulation is a result of an imbalance between photosynthetic activity and demand for
128 growth is discussed. We also provide insights into the mechanism of oil accumulation under
129 SL by reporting the proteomic and lipidomic analyses of SL-induced lipid droplets.

130

131

132 RESULTS

133

134 Experimental Setup and Choice of Light Intensity

135 To investigate the formation of carbon reserves in response to high light under
136 photoautotrophic conditions, it is paramount that light supply and penetrance is kept uniform
137 all throughout culture stages. When cultivating algae in batch cultures under current
138 laboratory conditions, the biomass increase leads to a decrease of light perceived per cell due
139 to shading in dense cultures. To achieve constant light perception, we cultivated *C.*
140 *reinhardtii* in continuous culture in photobioreactors (PBRs) monitored as turbidostats. This
141 allows for the cultures to be maintained at constant biomass levels (i.e. under a defined
142 physiological condition) throughout the course of the experiment with minimal differences
143 between cultures in terms of light exposure, and other parameters such as pH, nutrient or CO₂
144 supply.

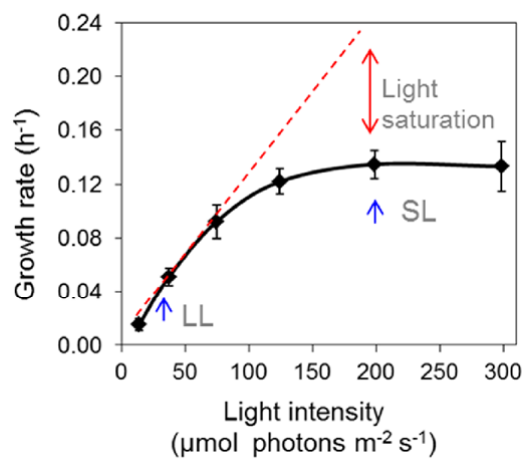
145 We first measured biomass productivity as a function of photon flux density (PFD)
146 (**Figure 1**). Non-limiting CO₂ condition was achieved by bubbling air containing 1.8% CO₂.
147 The growth rate increased progressively with rising PFD in the range of 0-100 $\mu\text{mol m}^{-2} \text{s}^{-1}$
148 but when light reached $>120 \mu\text{mol m}^{-2} \text{s}^{-1}$, a plateau in biomass growth was observed. Light
149 intensities above that threshold are thus saturating lights (SL). To evaluate the effects of light
150 intensity on carbon reserve formation, based on this first experiment, cells of
151 *Chlamydomonas* were cultivated first at a sub-saturating low light (LL, $37 \mu\text{mol m}^{-2} \text{s}^{-1}$) then
152 exposed to a saturating light of $200 \mu\text{mol m}^{-2} \text{s}^{-1}$ for 48 h (indicated as blue arrows in **Figure**
153 **1**). It is worth noting that the light intensity at which saturation of photosynthesis and growth
154 was obtained under this experimental set up (around $200 \mu\text{mol m}^{-2} \text{s}^{-1}$) may appear low
155 compared to what is generally used in most laboratory conditions (i.e. shake flasks with
156 mono-directional illumination). Such a low light saturation level resulted from the use of a
157 relatively low-density culture ($\text{OD}_{880 \text{ nm}} = 0.4$) and radial illumination (creating a
158 homogenous light inside the PBR). Since high light is a relative term, to avoid ambiguity, in
159 this study, we have instead used the term ‘saturating light (SL)’ throughout.

160 To dissect mechanistic differences in carbon reserve formation between cells exposed
161 to SL and those cultivated under N-starvation conditions, we setup four 1-L PBRs, two for
162 SL experiments, and two for the N-depletion experiments. To reflect real production
163 conditions, we employed a gradual N-depletion process rather than an abrupt N-starvation.
164 The experimental setups used and the parameters analysed in the rest of the work are outlined
165 in **Figure 2**.

Figure 1. Growth rate of biomass as a function of photon flux density in turbidostatic photobioreactors.

Strain CC-124 was cultivated in photobioreactors (PBRs), with a supply of 1.8% CO₂ in air. Growth rate was calculated as a rate of injection of fresh media to an existing culture while maintaining OD_{880nm} at 0.4 (equivalent to ~2 million cells mL⁻¹). The light intensities used in the rest of this study are indicated by blue arrows. Low light (LL) refers to 37 μmol m⁻² s⁻¹ and saturating light (SL) refers to 200 μmol m⁻² s⁻¹.

Data are means of two biological replicates and two technical replicates each. Error bars represent standard deviations.



1

166

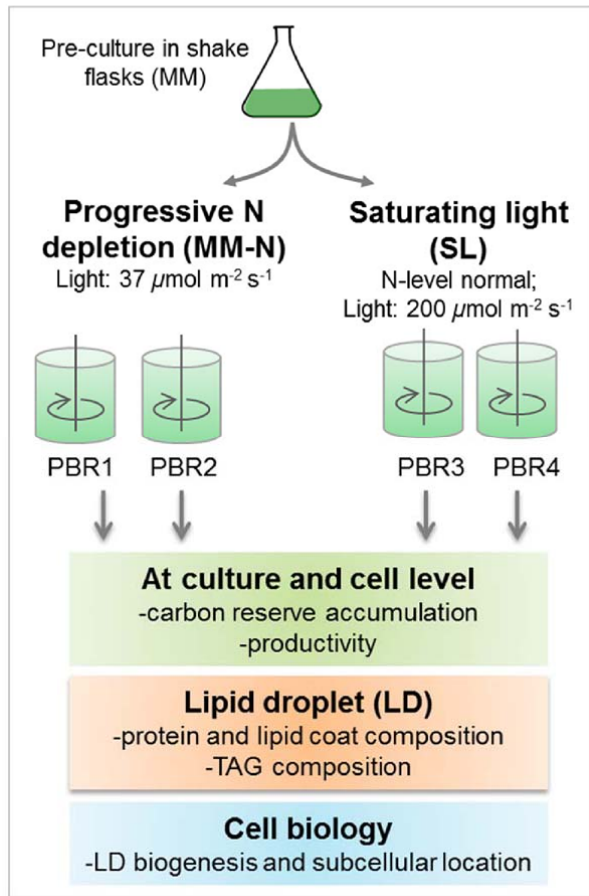
167 **Exposure to Saturating Light (SL) Increases Intracellular Oil and Starch Contents**

168 Quantification of intracellular oil and starch showed that SL-exposed cells accumulated both
169 starch and TAGs in a parallel manner (**Figure 3A**). Oil and starch accumulation was also

Figure 2. Experimental setup for the comparison of nitrogen starvation and saturating light conditions.

Strain CC-124 was maintained at a constant OD_{880nm} of 0.4 (equivalent to ~ 2 million cells mL^{-1}). SL: saturating light refers to a light intensity of $200 \mu mol m^{-2} s^{-1}$. Nitrogen starvation is achieved through progressive limitation and culture nitrogen level was measured.

Abbreviations: MM, minimal media; N, nitrogen; SL, saturating light; LD, lipid droplet; PBR, photobioreactor; OD, optical density; TAG, triacylglycerols.

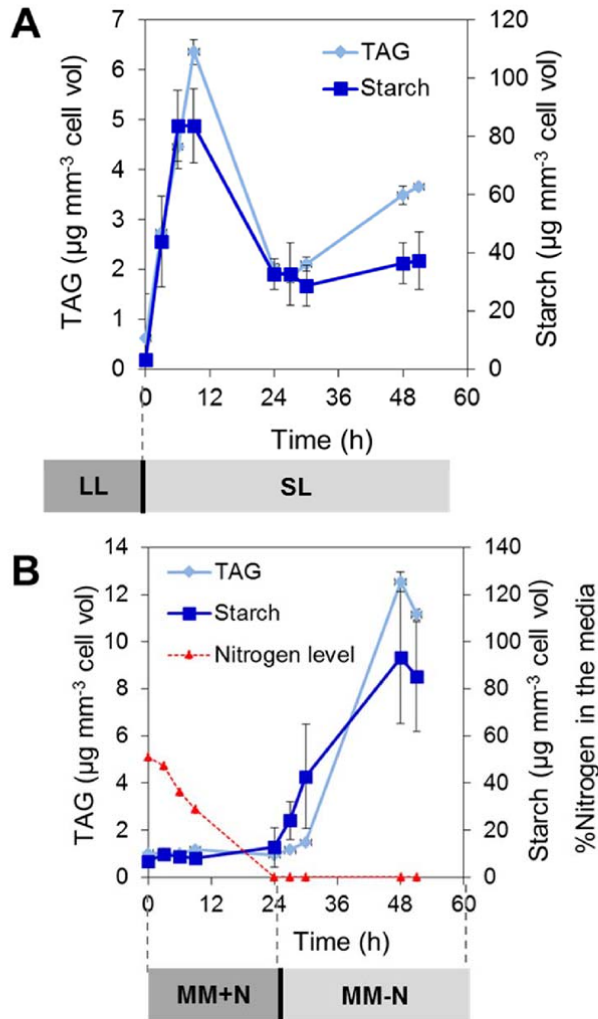


170 observed in N-starved cells under photoautotrophic PBR conditions (**Figure 3B**). Maximal
171 oil accumulation measured in SL-exposed cells ($\sim 6 \mu g mm^{-3}$ at 9 h) reached almost 50% of
172 the level determined for N-starved cells ($\sim 12 \mu g mm^{-3}$ at 24 h after N-depletion) and maximal
173 starch accumulation was similar ($\sim 80 \mu g mm^{-3}$ cells) under both conditions. A transient peak

Figure 3. Exposure to saturating light triggers oil and starch accumulation.

Cells were cultivated in photobioreactors in photoautotrophic conditions. Time zero in the SL and the N starvation experiment correspond to low light (LL) and +N controls, respectively. Data are means of two biological replicates with two technical replicates. Error bars represent standard deviations.

Abbreviations: MM, minimal media; N, nitrogen; TAG, triacylglycerols. SL, saturating light; LL, low light.



174 of TAG/starch accumulation was seen around 9¹ h upon SL exposure, followed by a drop and
175 stabilization upon 24 h. The stabilized level of reserves was still much higher than before SL
176 exposure, but lower than the maximal level observed under N-depletion. Moreover, an
177 increase in total fatty acids and also in carbon/nitrogen (C/N) ratio (from 4.8 to 5.7) were

178 observed in cells exposed to SL compared to those cultivated under LL (Supplemental
179 **Figure S1**), supporting the TAG quantification data (Figure 3).

180

181 **Oil and Starch Productivities are Higher in SL-Exposed Cultures than in N-Starved** 182 **Cultures**

183 Upon SL exposure, the specific growth rate of the *C. reinhardtii* culture grown in PBRs
184 progressively increased from 0.05 h^{-1} to a new steady state, which was reached at 0.12 h^{-1}
185 (**Figure 4A**). In sharp contrast, N depletion led to a progressive decrease in the growth rate
186 until it halted completely 6 h after full N-depletion (**Figure 4B**). Calculation of oil and starch
187 productivity by using specific growth rates with cellular oil and starch contents revealed that
188 compared to N starvation, SL-exposed cells achieved a 15 times higher productivity in TAG
189 ($\sim 6 \text{ mg L}^{-1} \text{ d}^{-1}$ vs. $\sim 0.4 \text{ mg L}^{-1} \text{ d}^{-1}$) and a 7 times higher productivity in starch ($\sim 70 \text{ mg L}^{-1} \text{ d}^{-1}$
190 $\text{vs. } 10 \text{ mg L}^{-1} \text{ d}^{-1}$) (**Figure 4C, D**). These results therefore show clearly that sustained
191 productivity of oil and starch could be achieved in PBRs under SL.

192

193

194 **SL-Exposed Cells Accumulate Oil in Lipid Droplets (LDs)**

195 Oil accumulation under SL exposure was found to form distinct LDs that were visible after
196 Nile red staining (**Figure 5A, B**). Interestingly, a significant portion of LDs in SL-exposed
197 cells were smaller than LDs under N starvation. This contrasted to those formed under N-
198 starvation, which were bigger and more abundant (**Figure 5C**). It is known that N-starved
199 *Chlamydomonas* WT cells accumulate LDs **mostly** at the junction of endoplasmic reticulum
200 and plastid envelopes (the so-called β -cyto-LDs) (Goodson et al., 2011). Here, we thus only
201 focused on the subcellular location of the LDs present in the SL-treated cells. This was
202 achieved by obtaining confocal microscopy images of several focal planes. For example,
203 when moving the focal plane from the top all the way down to the bottom of the cell, we
204 observed the presence or absence of LDs (**Figure 5D, E, F**). This contrasted with the
205 detection of chlorophyll autofluorescence. **These observations suggested that at least some of**
206 **the LDs formed were likely present inside the plastid (Figure 5D: white arrows point to one**
207 **example of this LD type)**. LDs that appeared to be cytosolic or associated to plastid
208 membranes in the same cell could also be seen. To confirm these observations, we further
209 examined the difference in the nature of LD populations under SL and N-starvation by
210 analysing the protein and lipid composition of isolated LDs.

211

Figure 4. Growth rates, oil and starch productivity under saturating light or nitrogen starvation.

A. Growth rates under saturating light (SL).

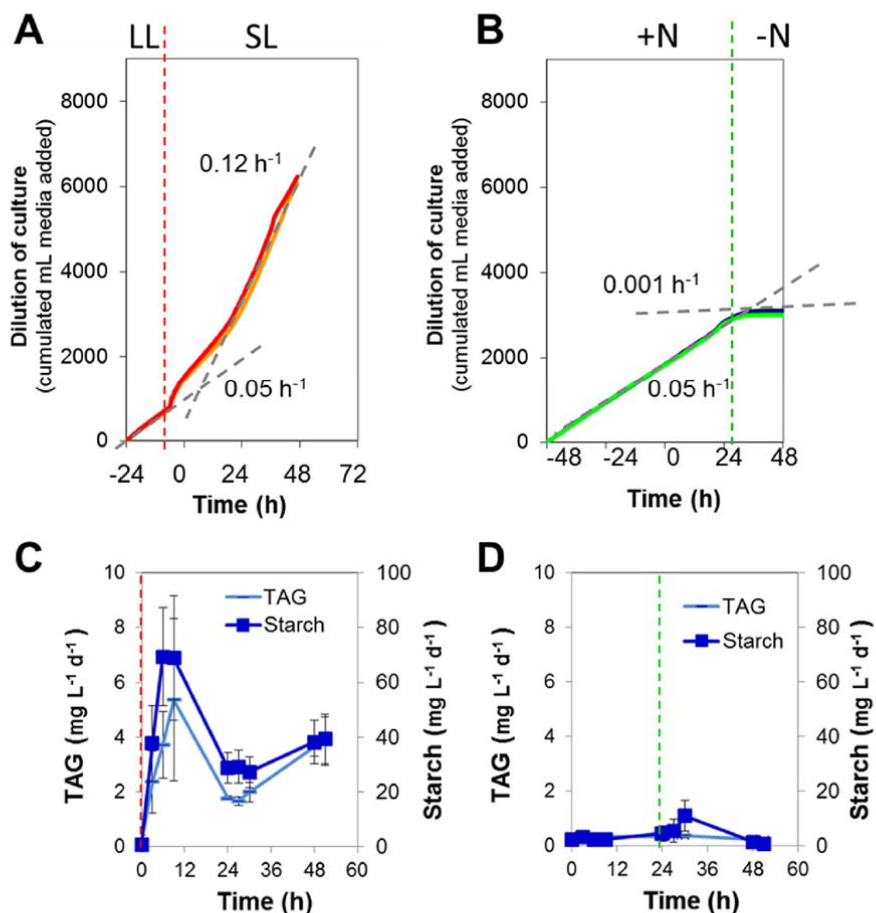
B. Growth rates under nitrogen (N) starvation.

C. Productivity of oil and starch under SL.

D. Productivity of oil and starch under N starvation.

Photobioreactors were first stabilized for 4 days, then exposed either to saturating light irradiance, or to nitrogen depletion. The growth rate was calculated based on the cumulated medium added to the photobioreactor culture to maintain a constant OD during cell culture. Red dotted lines indicate the moment SL is switched on, and green dotted lines indicate when nitrogen is completely depleted from the media. Data are means of two biological replicates and two technical replicates. Error bars denote standard deviations.

Abbreviations: MM, minimal media; N, nitrogen; SL, saturating light; LL, low light. L: liters of culture

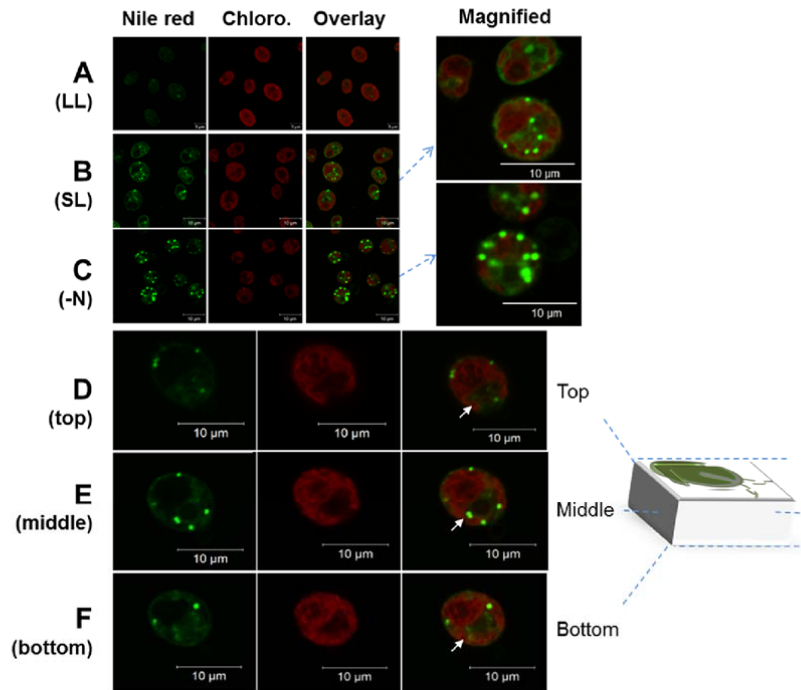


212 **LDs in SL-Exposed Cells Contain TAGs and Polar Lipids of Mostly Plastidial Origin**

213 To determine lipid and proteins present in LDs, we isolated LDs from both SL-exposed cells
 214 and N-starved cells cultivated in PBRs following 9 h SL-exposure (SL 9h), or 24 h N-
 215 starvation (MM-N 24h), respectively. These time points were chosen because they

Figure 5. Visualization of lipid droplets by Nile red staining and microscopy.

- A.** *Chlamydomonas* cells cultivated under normal conditions (MM+N/LL)
 - B.** *Chlamydomonas* cells after 9 h of saturating light (SL+N).
 - C.** *Chlamydomonas* cells after 24 h of N depletion (MM-N/LL).
 - D.** The 'top' focal plane of an image of Nile red stained SL-exposed cell
 - E.** The 'middle' focal plane of an image of Nile red stained SL-exposed cell
 - F.** The 'bottom' focal plane of an image of Nile red stained SL-exposed cell
- LD, lipid droplet; SL, saturating light; N, nitrogen.



216 correspond to the moment when the maximal cellular oil content was reached. After lipids
 217 were extracted from isolated LDs, polar and neutral fractions were separated by solid-phase
 218 extractions (SPE), and the proportion of each fraction was quantified after being converted to
 219 their fatty acid methyl esters (FAMES). LDs of N-starved cells contained 97% of neutral

Figure 6. Lipid composition of lipid droplets (LDs) isolated from SL-exposed cells and N-starved cells.

A. Proportion of membrane lipids versus triacylglycerols (TAG) in isolated LDs. Lipid amounts were determined by quantification of total fatty acids in each lipid fraction.

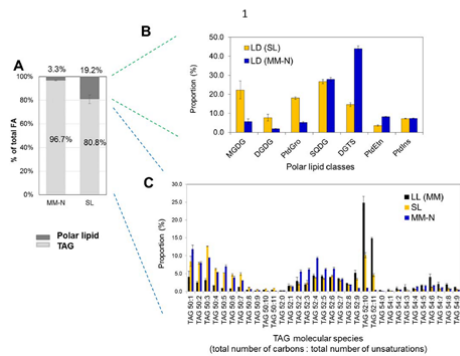
B. Proportion of major membrane lipid classes in isolated LDs. Content for each lipid class was determined by TLC.

C. Distribution of triacylglycerol (TAG) molecular species in isolated LDs.

Lipid droplets were isolated from cells being N-starved for 24 h (corresponding to 48 h in **Figure 3**) or from cells exposed to saturating light ($200 \mu\text{mol m}^{-2} \text{s}^{-1}$) for 9 h. These time points were chosen because they represent the peak of oil accumulation under either treatment.

Data are means of two biological and two technical replicates, with standard deviations shown.

Abbreviations: FA, fatty acid; TAG, triacylglycerol; MM-N, minimal media under nitrogen starvation; MGDG, monogalactosyldiacylglycerol; DGDG, digalactosyldiacylglycerol; PtdGro, phosphatidylglycerol; SQDG, sulfoquinovosyldiacylglycerol; DGTS, diacylglycerol *N,N,N*-trimethylhomoserine; PtdEtn, phosphatidylethanolamine; PtdIns, phosphatidylinositol; LD, lipid droplet; ER, endoplasmic reticulum.



220 lipids and 3% polar lipids whereas those of SL-exposed cells contained only 81% neutral
 221 lipids and 19% polar lipids (**Figure 6A**). In a typical LD topology, neutral lipids are covered
 222 by a polar membrane shell (Jolivet et al., 2013). Since smaller LDs contain a higher
 223 proportion of polar membrane lipids than larger LDs, this suggests that the LDs in SL-

224 exposed cells are smaller than those induced by N-starvation, which was consistent with
225 microscopic examinations (**Figure 5**).

226 The polar lipids of LDs isolated from SL-exposed cells showed a high content in
227 MGDG and SQDG, followed by PtdGro and DGTS, then DGDG, PtdIns and PtdEtn (**Figure**
228 **6B**). This composition clearly contrasts with the LDs of N-starved cells, where DGTS and
229 SQDG are the major polar lipid species (**Figure 6B**), which corroborates previous
230 observations (Wang et al., 2009). With the exception of PtdIns, molecular species within a
231 particular lipid class also differed between these two LD types (**Supplemental Figure S2**).
232 LDs induced by SL contained a high proportion (~70%) of lipids unique to photosynthetic
233 membranes (i.e. MGDG, DGDG, SQDG), whereas LDs of cells in the N-starvation condition
234 contained ~60% of extra-plastidial lipids (DGTS and PtdEtn).

235 TAG molecular species present in the two LD types were also found to differ.
236 Compared to TAG species present in cells under optimal growth condition (i.e. low light and
237 nutrient replete condition; LL), SL-induced LDs contained significant higher proportion of all
238 TAG50 species, yet with significant reductions in TAG species rich in polyunsaturated fatty
239 acids (TAG52:10 and TAG52:11) (**Figure 6C**). Interestingly, the above polyunsaturated
240 TAG species are present in higher proportions in LDs induced by SL than those triggered by
241 N starvation (**Figure 6C**).

242

243 **LDs of SL-Exposed Cells Contained Higher Proportions of Proteins of Plastidial Origin**

244 In order to gain further insights in LD formation under SL, we performed a proteomic
245 analysis to compare the protein compositions of LDs accumulating in SL to those isolated
246 from N-starvation conditions. Total proteins associated to LDs isolated under SL or -N
247 conditions were loaded and separated on a SDS-PAGE. Protein extracts were loaded based on
248 an equal amount of total lipids. LDs formed under SL showed a distinct protein composition
249 compared to those of N-induced LDs (**Figure 7A**). Proteomic analyses by LC-MS/MS
250 identified 222 proteins associated to LDs in SL-exposed cells, and 303 proteins in LDs
251 formed under N-starvation (**Figure 7B; Supplemental Table S1A, B**). To be stringent, we
252 kept only those proteins for which ≥ 2 unique peptides and ≥ 2 specific spectral counts (SSC)
253 were identified. Proteins were ranked according to their estimated relative abundance within
254 each LD biogenesis condition. Comparisons between the two proteomes showed that 148
255 proteins are identified in both proteomes (**supplemental Table S1C**), whereas 74 unique
256 proteins were identified in SL-induced LDs (**supplemental Table S1D**), a large portion of
257 which (31/74) were of plastidial origin based on a prediction using the green algae protein-

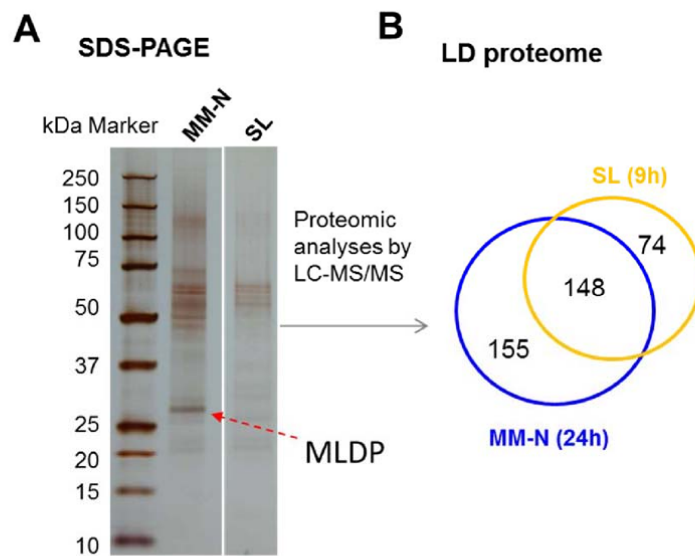
Figure 7. Comparison of proteomic composition of lipid droplets (LDs) isolated from cells subjected to saturating light (SL) or N-starvation.

A. Silver nitrate-stained SDS-PAGE of total proteins extracted from purified LDs.

B. Venn diagram showing the total number of proteins associated to LDs under each condition. Only proteins with ≥ 2 peptides and ≥ 2 specific spectra counts were retained for analyses.

LDs were purified from cultures either after 24 h nitrogen depletion, or from cultures after being exposed to saturating light for 9 h.

Abbreviations: LD, lipid droplet; SL, saturating light; kDa, kilo daltons; LC-MS/MS: liquid chromatography – tandem mass spectrometry; MM, minimal media; N, nitrogen.



1
2
258 adapted algorithm PredAlgo (Tardif et al., 2012). We detected significant amount of
259 ‘plastidial’ proteins in both LD preparations, but we could not tell if these proteins are
260 contaminations or are they integral part of the LD proteome. These questions should be
261 addressed in the future through studies of protein subcellular localizations.

262 The identity and annotation for the top 30 ranked proteins associated to LDs isolated
263 from SL-exposed cells are listed in **Table 1**. Proteins common to both LD isolates include the
264 major lipid droplet protein (MLDP), the diacylglyceryl-*N,N,N*-trimethylhomoserine synthesis
265 protein (BTA1), the cyclopropane-fatty-acyl-phospholipid synthase (CFA2), an α/β
266 hydrolase, a glycosyl hydrolase (GHL1), a long chain acyl-CoA synthetase (LCS2), a β -
267 tubulin 1 (TUB1), a lysophospholipid acyltransferase (LPLAT), and one of the components
268 of the plastid lipid reimport machinery (TGD2) (**Supplemental Table S1C; Table 2**). These
269 proteins have been found to be present in all three previously reported LD proteomics studies
270 (Moellering and Benning, 2010; Nguyen et al., 2011; Tsai et al., 2015). With the exception of
271 TGD2, all of the above-mentioned top-ranked proteins in N-induced LDs are not the same
272 major proteins in SL-LDs, i.e. their ranks in SL-LDs being relatively inferior to those in N-
273 induced LDs (**Table 2**). These rankings were calculated based on a computed calculation of
274 total number of SSCs and values of exponentially modified protein abundance index
275 (emPAI), and can be used to evaluate the relative abundance of each protein in a sample.

276 Among the 74 proteins found only in LDs of SL-origin, of particular note is the
277 presence of relatively large proportion (~45%) of proteins of plastidial origin, including the
278 Proton Gradient Regulation Like1 (PGRL1), the Plastid Lipid Associated Protein 8 (PLP8
279 Cre14.g611700), and also a 2-methyl-6-phytyl-1,4-benzoquinone/2-methyl-6-solanyl-1,4-
280 benzoquinone (MPBQ/MSBQ) methyltransferase (VTE3) (**Supplemental Table S1D**).

281

282

283 **DISCUSSION**

284

285 In this study, we showed that saturating light (SL) can increase cellular oil content while
286 maintaining cell turnover and biomass growth, thus leading to a sustainable production of
287 carbon reserves. This clearly contrasts with the well-characterized N starvation-induced oil
288 accumulation, where oil productivity remained low despite achieving a higher cellular TAG
289 content. We further showed that SL induces formation of smaller LDs than those formed
290 under N starvation. The SL-induced LDs had a lipid and protein coat enriched in components
291 of plastidial origin, thus LDs formed under SL are distinct from those formed under N-
292 starvation. This serves as the first report on LD composition beyond the model of N-
293 starvation-induced LDs in *C. reinhardtii*.

294

295 **Origin of TAGs under Saturating Light**

296 An increase in total fatty acids was seen together with an increase in C/N ratio in cells
297 exposed to SL (**supplemental Figure S1**). The positive correlation between TAG levels and
298 C/N ratio has also been observed previously in the seeds of Arabidopsis when the plant is
299 grown under increasing irradiance (Li et al., 2006). Thus, after being exposed to SL, the cells
300 re-adjust their metabolism to store the extra carbon and energy as energy-dense materials i.e.
301 starch and oil. These storage compounds provide a temporary reservoir to accommodate the
302 extra fluxes of ATP and reducing powers thereby ensuring cell energetic homeostasis. This
303 increased de novo fatty acid synthesis is further reflected in the changes in total fatty acid
304 compositions before and after SL exposure (**Figure S1D**; and **Figure 6C**), i.e. increased
305 proportion of saturated C16 fatty acid and a reduction in polyunsaturated fatty acid species.
306 Increased C flow to TAG synthesis under high light have also already been recently reported
307 in the heterokont alga Nannochloropsis, in which activities of acetyl-CoA carboxylase
308 (ACCase) and diacylglycerol acyltransferase (DGAT) are significantly increased following a
309 transition from low to high light cultivation conditions (Ma et al., 2016).

310 In addition to the increased C flow to fatty acid synthesis, the composition of total
311 polar lipids was altered following exposure to SL. SL-treated cells contained a reduced
312 proportion of monogalactosyldiacylglycerol (MGDG) and increased proportion of
313 digalactosyldiacylglycerol (DGDG) and diacylglycerol *N,N,N*-trimethylhomoserine (DGTS),
314 with the other major lipids remaining constant (**Supplemental Figure S1C**). Taken together,
315 these data suggest that under SL, both *de novo* fatty acid synthesis and membrane lipid

316 remodelling contribute to TAG formation, a phenomenon similar to what is occurring in cells
317 starved for nitrogen.

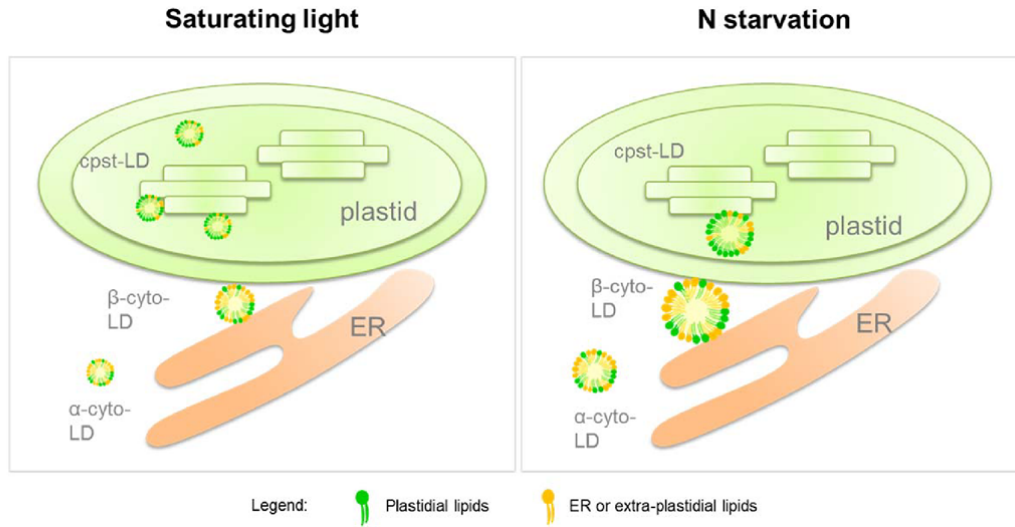
318

319 **Biogenesis and Physiological Functions of Lipid Droplets under Saturating Light**

320 Most of our knowledge of LD biology in *C. reinhardtii* is gained from studies of LDs
321 induced by N starvation. Three types of LDs (α -cyto-LDs, β -cyto-LDs, cpst-LDs) have been
322 distinguished in *C. reinhardtii* upon N starvation; the types and relative abundance of each
323 LD population differs depending on the cultivation condition and on the genotype (Fan et al.,
324 2011; Goodson et al., 2011). For example, it has been observed that optimally growing cells
325 contain a few α -cyto-LDs (i.e. free cytosolic LDs), whereas upon N starvation, wild-type
326 strains of *C. reinhardtii* store oil mostly in β -cyto-LDs (i.e. LDs formed at the junction
327 between ER and plastid envelop), whereas the starch-less mutant *bafJ5* accumulates cpst-LDs
328 (i.e. chloroplast-located LDs) in addition to β -cyto-LDs (Goodson et al., 2011). Here we
329 observed that SL can also trigger LD formation. Part of the LDs seem to be inside the plastids
330 (cpst-LDs), and part of them being outside the plastid but in most cases seem to be associated
331 to the plastid envelopes (β -cyto-LDs)(**Figure 8**). Lipidomics analyses showed that LDs
332 formed under SL exposure are made of a mixture of saturated and polyunsaturated TAGs,
333 and covered by protein- and lipid-coat rich in components of plastidial origin. The presence
334 of a plastidial TAG biosynthesis pathway is not surprising. It has previously been observed in
335 the N-starved starch-less mutant *bafJ5* (Fan et al., 2011; Goodson et al., 2011), and can also
336 be deduced by the subcellular targeting of key TAG enzymes in the plastid (Li-Beisson et al.,
337 2015).

338 The protein and lipid composition of the LD coat further demonstrated that SL-
339 induced LDs consist of components of mostly plastidial origin. For example, besides
340 common proteins, SL-induced LDs were found to contain a significant subset of plastid-
341 resident proteins including PGRL1, PLP8 and VTE3. PGRL1 is a major component of cyclic
342 electron flow (CEF) in *C. reinhardtii*, and has been proposed to supply additional ATP for
343 photosynthesis, particularly in conditions of high ATP demand (Tolleter et al., 2011; Dang et
344 al., 2014). The PGRL1 deficient mutant (*pgrl1*) has been recently reported to accumulate less
345 neutral lipids under N starvation, and it was suggested that CEF supplies ATP for lipid
346 biosynthesis during N-starvation (Chen et al., 2015). The association of PGRL1 with LDs of
347 SL-exposed cells expands its role in supplying ATP for TAG synthesis under SL conditions.
348 Interestingly, homologs of the two other proteins (PLP8 and VTE3) in the model plant
349 *Arabidopsis thaliana* and have been found to be associated with plastoglobules (PGs), a type

Figure 8. A model on LD biogenesis in cells exposed to saturating light or N-starvation.
 Three types of LDs were drawn, partly based on observations made in this study, and partly based on that Goodson et al (Goodson et al., 2011).
 Cpst: chloroplast; cyto: cytoplasm



350 of LDs specific to plant plastids (Kessler and Vidi, 2007). PLP8 is known to play a structural
 351 role, whereas VTE3 is required for vitamin E synthesis and recycling (Martinis et al., 2013).
 352 Vitamin E synthesis is essential for photo-adaptation to survive in higher irradiance. The

353 presence of VTE3 in isolated SL-LDs supports the view that LDs play a photo-protective
354 roles via synthesizing oil-soluble vitamins.

355 We conclude that a significant sub-population of SL-induced LDs is associated to the
356 chloroplast (cpst-LDs and β -cyto-LDs), consistent with our microscopic observations. Under
357 SL exposure, wild-type strains of *Chlamydomonas* would mostly form cpst-LDs. The
358 formation of cpst-LDs have previously been observed in the starch-less mutant *bafJ5* during
359 N starvation (Goodson et al., 2011). Therefore, cpst-LDs are formed either in the absence of
360 the ‘starch’ (*bafJ5* mutant), or under a high fluence rate, extra photosynthetic products being
361 diverted to the formation of LDs inside the plastid. Both situations create an imbalance in the
362 ‘supply and demand’ of reduced carbon (discussed in the next section) and favour the
363 formation of plastidial LDs, a convenient and local solution. However, in the absence of the
364 protein/lipid composition data for cpst-LDs of the starch-less mutant, we cannot assert that
365 the two cpst-LDs are of the same nature, and this question should be investigated in the
366 future.

367 It should bear in mind that LD isolates in each condition most likely represent a
368 mixture of LDs of chloroplast-LDs (cpst-LDs) and cytosolic-LDs (cyto-LDs). The difference
369 in protein relative abundance (i.e. as shown by rankings)(**Table 2**) could be because these
370 proteins are indeed present in much less concentration in all sub-population of LDs induced
371 by SL than those triggered by N-starvation, or alternatively, it could be that these proteins
372 were only associated with a specific sub-population of LDs in the SL-exposed cells. This and
373 other possibilities can only be answered once the subcellular localization information is
374 available for these proteins under the different culture conditions.

375

376 **Imbalance Between Photosynthesis and Growth Governs Reserve Accumulation**

377 Previous studies have shown that oil accumulation is triggered by conditions which impair
378 cell growth (Merchant et al., 2012; Liu and Benning, 2013). Increasing light intensity has also
379 been reported as a means to increase oil content when combined with N starvation (Klok et
380 al., 2013; Kandilian et al., 2014). The latter two studies have shown that in conditions of N
381 starvation, high light participates to increase the energy imbalance, resulting in a higher TAG
382 storage in the heterokont *Nannochloropsis oculata* and the green microalga *Neochloris*
383 *oleoabundans*. The current study provides a detailed report on the effect of light on reserve
384 accumulation under optimal growth conditions for the model microalga *C. reinhardtii*. We
385 found that SL-exposed cells accommodate an excess of light energy by storing reduced
386 carbon in the forms of starch and neutral lipids.

387 The impact of high light on storage reserve accumulation is sometimes considered as
388 a consequence of a ‘light stress’ effect. We observed a ‘burst’ in oil/starch content following
389 SL-exposure. This suggests that cells respond to SL in two phases: an initial strong response,
390 followed by an acclimated phase. This initial burst is most likely **due to a combined stress**
391 **response with an increased C flux toward reserve formation at the beginning**, followed by a
392 metabolic adaptation to the increased irradiance. As cultivation under SL proceeded,
393 acclimated cells synthesized higher amounts of carbon reserves simultaneous to an increased
394 growth rate. Thus saturating light combined with a non-limiting CO₂ supply induces
395 significant oil accumulation in *C. reinhardtii* in conditions that supports maximal growth. We
396 therefore conclude that oil accumulation is not necessarily linked to a stress effect inducing
397 growth impairment, but may occur in conditions of maximal growth.

398 Upon steady-state SL exposure, the photosynthetic capacity may exceed the cell
399 division and growth capacity, thus creating an imbalance between the formation of
400 photosynthetic products and the capacity for their direct consumption. The cellular
401 metabolism would thus be re-adjusted to store the extra energy as energy-dense materials i.e.
402 starch and oil. These storage compounds provide a temporary reservoir to accommodate the
403 extra fluxes of ATP and reducing power thereby ensuring cell energetic homeostasis. Based
404 on these data, we propose a more general model in which starch and oil accumulations are
405 triggered when an imbalance between photosynthetic CO₂ fixation and growth occurs
406 (**Figure 9**). Such an imbalance may occur in conditions where growth is primarily affected
407 (such as nutrient starvation, heat, salinity or chemical treatment...), but may also occur in
408 conditions of SL where photosynthetic CO₂ fixation exceeds the ability of algae to grow and
409 replicate. The large increase in neutral lipid and starch productivity achieved under SL clearly
410 points out the biotechnological advantage to increase reserve accumulation under conditions
411 not compromising growth in green microalgae.

412

413 **MATERIALS AND METHODS**

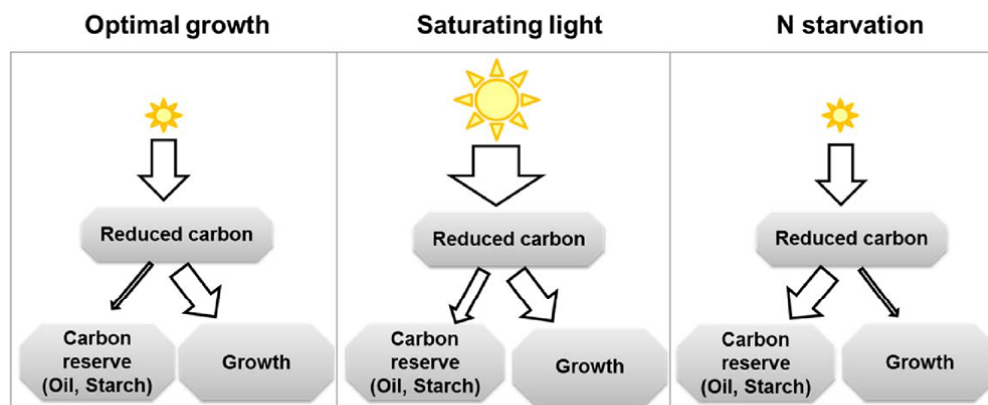
414

415 ***C. reinhardtii* Strains and Pre-Cultures**

416 The wild-type *C. reinhardtii* strain CC-124 (*mt- nit1 nit2*) was used throughout this study.
417 Cells were usually maintained in Tris-Acetate-Phosphate (TAP) medium (Harris, 2001) in
418 Erlenmeyer flasks at 25°C with shaking at 120 rpm under constant illumination (150 μmol
419 photons m⁻² s⁻¹). For photoautotrophic growth, cultures grown in minimal medium (MM)
420 were kept under identical conditions with additional supply of 1.8% CO₂ in air (Cagnon et al.,

Figure 9. Carbon reserve formation in *Chlamydomonas* in response to energy imbalance: a model

During normal growth (low light, nutrient-replete conditions), *Chlamydomonas* cells convert most of the solar energy they have captured through the photosystems and fixed as organic compounds, to support biomass growth (cell division); only a small fraction is used to make temporary carbon reserves (starch and oil). Creating an energy imbalance either through an increased input of energy (saturating light with respect to biomass growth), or a decrease in energy use (through blocking growth via nitrogen starvation) results in re-allocation of the excess of energy to the synthesis of reserve compounds (oil and starch).



421 2013). Cell numbers were counted using a Beckman-Coulter multisizer (Beckman Coulter).¹
 422 Cellular concentration was determined as number of cells per mL of culture, or total cellular
 423 volume (μm^3) per mL of culture.
 424

425 **Cultivation in Photobioreactors (PBRs)**

426 PBR cultures were cultivated in MM media in automated Biostat A Plus PBR systems
427 (Sartorius Stedium) as described previously (Dang et al., 2014). Cells were maintained at a
428 constant OD_{880nm} (= 0.4) throughout experimentation. Specific growth rates were determined
429 from the measurement of fresh medium added to the turbidostat to maintain a constant
430 biomass concentration. All the PBRs were stirred at a constant 300 rpm.

431

432 **Quantification of Starch**

433 Starch were isolated and quantified based on the protocol described in (Klein and Betz,
434 1978). Cells were harvested by centrifugation of *Chlamydomonas* cells at 1000 g for 3 min.
435 Cellular pellets were resuspended in 1 mL methanol, and centrifuged again for 3 min at 1000
436 g to remove all chlorophyll. The methanol washed pellet was air-dried under a fume-hood,
437 and subsequently resuspended in 400 µL of distilled water, samples were then autoclaved for
438 20 min at 121°C. Amyloglucosidase (0.2 U - Roche) was added and samples were incubated
439 for 1 h at 60°C. Samples were then centrifuged to pellet particulate matter. Glucose was
440 measured with an YSI2700 select sugar analyser (YSI Life Sciences) using commercial
441 glucose as a standard.

442

443 **Isolation of Lipid Droplets (LDs)**

444 In order to isolate low-abundant LDs, a previously established *Chlamydomonas* LD isolation
445 protocol (Nguyen et al., 2011) was used with the following minor changes. A desktop ultra-
446 centrifuge replaced the standard ultracentrifuge, and smaller 5-mL ultracentrifuge tubes were
447 used to decrease the surface area of the lipid pad, and increase the ease with which the lipid
448 pad is completely recovered. Additionally, to avoid loss of material the hexane wash was
449 omitted and during the final wash a sucrose-free buffer was used to replace the 0.4 M sucrose
450 buffer. In the final step, a sucrose free buffer floats above all other buffers and allows for
451 easier isolation of the final washed LDs.

452

453 **Lipid Extractions, Quantification of Lipid Classes by Thin Layer Chromatography**
454 **(TLC) and Lipid Molecular Species Analysis Using an Ultra-Performance Liquid**
455 **Chromatography – Tandem Mass Spectrometry (UPLC-MS/MS)**

456 A modified Bligh and Dyer method (Bligh and Dyer, 1959) was used to extract lipids.
457 Samples were initially dissolved by vortexing in 1 mL quenching solution (1 mM EDTA,
458 0.15 M acetic acid) in an 8-mL glass tube with a Teflon screw-cap. Three mL of

459 methanol:chloroform (2:1 v/v) was added, if samples were to be used for LC-MS/MS at this
460 stage internal standards TAG51:0 (comprised of 17:0/17:0/17:0 fatty acids) and PtdEtn34:0
461 (comprised of 17:0/17:0 fatty acids) were added. Samples were then vortexed for 10 min, 1
462 mL of chloroform and 0.8 mL of KCl (0.8% w/v) was added, and samples were vortexed
463 again for 10 min. Phases were separated by centrifugation at 1000 g for 2 min at 4°C. The
464 lower phase was then isolated and transferred to a new clean glass tube. To the remaining
465 phase, 1 mL of hexane was added to extract again the remaining lipids. Phases were then
466 separated by centrifugation at 1000 g for 2 min at 4°C. The upper phase containing lipids was
467 then transferred to the chloroform extract using a glass Pasteur pipette. The combined
468 chloroform and hexane extracts were then dried under a flow of nitrogen and re-suspended in
469 a mixture of chloroform:methanol (2:1 v/v) for subsequent analyses.

470 To analyse TAG content in cells and major polar lipid species, total lipids extracted
471 by the above protocol were processed using an automated “High-Performance Thin-Layer
472 Chromatography” platform (HP-TLC, CAMAG). The detailed TLC method has been
473 described in (Siaut et al., 2011). Lipid molecular species were analysed by LC-MS/MS and
474 conditions were detailed in (Légeret et al., 2016).

475

476 **Generation of Fatty Acid Methyl Esters (FAMES) and Quantification by Gas** 477 **Chromatography-Flame Ionization Detector (GC-FID)**

478 Conversion of total lipids to their fatty acid methyl esters were carried out as described
479 previously (Siaut et al., 2011). A fraction of extract was mixed in an 8-mL glass tube with 1
480 mL of methanol containing 5% H₂SO₄ v/v, to which 10 µL butyrate hydroxyl-toluene (BHT)
481 (1% v/v) and 5-25 µg of TAG(17:0/17:0/17:0) standard were added. Each sample was
482 vortexed for 30 sec, and heated to 85°C for 90 min. After cooling down to room temperature,
483 1.5 mL 0.9% NaCl (w/v) was added together with 1 mL hexane. Samples were vortexed for
484 10 min, and centrifuged at 1000 g for 2 min at 4°C. The upper (organic) phase was then
485 isolated with a clean glass Pasteur pipette, and evaporated to dryness under a stream of
486 nitrogen. Samples were finally resuspended in hexane. Fatty acid methyl ester species were
487 separated by the use of a ‘TRACE GC Ultra’ gas chromatograph (Thermo Fisher Scientific,
488 USA) using a polar TR-WAX column (Thermo Fisher Scientific, 30m x 0.25mm). Detailed
489 GC conditions have been described in (Nguyen et al., 2013).

490

491 **Protein Extraction, SDS-PAGE and Proteomic Analysis**

492 Proteins were extracted from isolated LDs by addition of cold acetone (80% v/v) and SDS
493 (0.3% v/v). Extracted proteins were separated on SDS-PAGE following standard protocols
494 (Sambrook and Russell, 2001). Proteins were then stained with a silver nitrate solution for 30
495 min. For proteomics analysis, samples in biological duplicates were concentrated at the top of
496 a NuPage precasted gel (Invitrogen) (“stacking” migration). Bands were cut and submitted to
497 LC-MS/MS analysis following the same procedure as reported in (Nguyen et al., 2011)
498 except for the following: the LC-MS/MS experiment were performed on a LTQ-Orbitrap
499 Velos Pro (Thermo Fisher Scientific) coupled to an Ultimate 3000 LC system. The *C.*
500 *reinhardtii* protein database used for Mascot (v2.4, 4, Matrix Science) searches was
501 constituted of the models downloaded from Phytozome (release 169_v4.3,
502 <http://phytozome.jgi.doe.gov/>), plus mitochondrion and plastid-encoded proteins from NCBI
503 (total of 17191 entries). Acetyl (protein *N*- α -acetylation) and methionine oxidation were set
504 as variable modifications and carbamidomethyl cysteine as fixed modification. Two mis-
505 cleavages were allowed. Mascot search results were automatically filtered as previously
506 described (Nguyen et al., 2011) with the IRMa 1.31.1 version software (Dupierris et al.,
507 2009).

508

509 **Microscopy**

510 Samples were stained first with Nile red (Sigma) at a final concentration of 1 $\mu\text{g mL}^{-1}$ (from a
511 stock solution of 1 mg mL^{-1} in methanol) for 10 min in the dark, then imaged with a Confocal
512 microscope TCS SP2 using an 63xoil immersion objective (Leica; Germany). The Nile red
513 signal was captured using a laser excitation line at 488 nm; and emission was collected
514 between 554-599 nm. Chlorophyll autofluorescence was measured by excitation at 635 nm
515 and emission captured between 650-714 nm. Pseudo colours for images were obtained using
516 the ZEN (Carl Zeiss) software.

517

518 **Acknowledgements**

519 Hugh Douglas Goold thanks The University of Sydney for an Australian Postgraduate Award
520 and the Paul Finlay scholarship. Yuanxue Liang thanks China Scholarship Council (CSC) for
521 a Postgraduate Award. We thank Patrick Carrier for assistance in running and maintaining
522 PBRs. Work in the authors’ laboratory is supported by the French Agence Nationale pour la
523 Recherche (ANR-Diesalg: ANR-12-BIME-0001-02). The support of A*MIDEX project
524 funded by the “Investissements d’Avenir” and the Proteomics French Infrastructure (ANR-
525 10-INBS-08-01) are also acknowledged. Support for the microscopy equipment was provided

526 by the Région Provence Alpes Côte d'Azur, the Conseil Général des Bouches-du-Rhône, the
 527 French Ministry of Research, the CNRS and the CEA. We also thank the European Union
 528 Regional Developing Fund (ERDF), the Région Provence Alpes Côte d'Azur, the French
 529 Ministry of Research and the CEA for funding the HélioBiotec platform.

530

531

532 **Tables**

533

534 **Table 1. Identity and abundance of the top 30 proteins found to be associated to LDs**
 535 **isolated from cells exposed to saturating light (SL) for 9 h.**

536 \N: no annotation is available.

537 Abbreviations: SL, saturating light; SSC, specific spectra count; emPAI: exponentially
 538 modified protein abundance index. The rankings were calculated based on a computed
 539 calculation of total number of SSCs and values of exponentially modified protein abundance
 540 index (emPAI), and can be used to evaluate the relative abundance of each protein in a
 541 sample.

542

543

544

ID (Phytozome or JGI)	Symbol	Defline	SSC	emPAI	Rank
Cre61.g792450.t1.2	\N	\N	48.5	0.765	1
Cre07.g324200.t1.1	BTA1	Diacylglyceryl- <i>N,N,N</i> -trimethylhomoserine synthesis protein	40.5	2.071	2
Cre01.g013700.t1.1	\N	\N	24.5	7.566	3
gi 41179057 ref NP_958414.1	\N	ATP synthase CF1 beta subunit [Chloroplast encoded]	24	1.978	4
gi 41179032 ref NP_958388.1	\N	Photosystem II 47 kDa protein [Chloroplast encoded]	24	1.452	5
Cre17.g698000.t1.1	ATP2	Mitochondrial F1F0 ATP synthase, beta subunit	21	1.683	6
Cre12.g540550.t1.2	α/β hydrolase	\N	21	1.523	7
Cre05.g241950.t1.1	\N	\N	20.5	6.462	8
Cre41.g786600.t1.1	AAA1	Plastidic ADP/ATP translocase	20.5	1.239	9
gi 41179063 ref NP_958420.1	\N	Photosystem II protein D2 [Chloroplast encoded]	20	1.713	10

Cre04.g229300.t1.2	RCA1	Rubisco activase	19	2.027	11
Cre12.g498600.t1.1	\N	Eukaryotic translation elongation factor 1 alpha	18	1.612	12
gi 41179065 ref NP_958422.1	\N	Photosystem II 44 kDa protein [Chloroplast encoded]	17.5	1.394	13
Cre09.g405500.t1.2	MLDP	Major lipid droplet protein	17	4.425	14
gi 41179003 ref NP_958358.1	\N	Cytochrome f [Chloroplast encoded]	16.5	2.316	15
Cre09.g398700.t1.1	CFA2	Cyclopropane-fatty-acyl-phospholipid synthase	16	1.365	16
Cre09.g386650.t1.1	ANT1	ADP/ATP carrier protein, mitochondrial	14.5	2.047	17
Cre16.g672650.t1.1	\N	Mitochondrial substrate carrier protein, possible 2-oxoglutarate/malate carrier	14	2.618	18
Cre02.g081050.t1.1	FAP24	Flagellar Associated Protein	14	0.965	19
Cre29.g778950.t1.1	FMG1-B	Flagella membrane glycoprotein, major form	14	0.104	20
Cre03.g171050.t1.2	GHL1	Glycosyl hydrolase	13	0.943	21
Cre02.g130650.t1.1	\N	\N	13	0.583	22
Cre01.g002500.t1.1	COP2	Chlamyopsin, light-gated proton channel rhodopsin	12.5	2.709	23
Cre17.g738050.t1.1	AGG4	Flagellar membrane protein, paralog of AGG2	12	2.590	24
Cre17.g734300.t1.2	\N	\N	12	0.411	25
Cre15.g638500.t1.1	CYC1	Ubiquinol:cytochrome c oxidoreductase cytochrome c1	11.5	1.561	26
Cre03.g172300.t1.1	\N	Mitochondrial phosphate carrier protein	10.5	0.901	27
Cre01.g025350.t1.1	FAP235	Flagellar Associated Protein	10	2.777	28
Cre03.g196900.t1.1	\N	\N	10	1.813	29
Cre23.g766250.t1.1	LHCBM1	Chlorophyll a/b binding protein of LHCBM1	10	1.396	30

545

546

547 **Table 2.** A short list of key proteins consistently found in all 3 previously published
548 proteomic studies of LDs isolated from *C. reinhardtii*.

549 Note: these proteins have demonstrated roles related to LD biology, and the cited previous
550 proteomics studies are (Moellering and Benning, 2010; Nguyen et al., 2011; Tsai et al.,
551 2015).

552 Abbreviations: MM, minimal medium; N, Nitrogen; SL, saturating light; Score, Mascot score
 553 (average from two replicates); SSC, specific spectra count (average from two replicates).

Synonym	Defline	LDs (MM-N)				LDs (SL)			
		Peptides	SSC	Score	Rank	Peptides	SSC	Score	Rank
BTA1	Diacylglyceryl- <i>N,N,N</i> -trimethylhomoserine synthesis protein	41	94	2120	1	24	41	1198	2
MLDP	Major lipid droplet protein	19	75	1467	2	13	17	982	14
α/β hydrolase	alpha beta hydrolase	28	63	1832	3	13	21	970	7
LCS2	Long chain acyl-CoA synthetase	32	54	1646	4	7	7	323	59
GHL1	Glycosyl hydrolase	23	46	1268	5	11	13	597	21
CFA2	Cyclopropane-fatty-acyl-phospholipid synthase	19	34	1147	6	10	16	597	16
LPLAT	Lysophospholipid acyltransferase	20	33	966	7	4	4	213	129
TUB1	Beta tubulin 1	15	16	673	23	6	6	272	85
TGD2	Permease-like component of an ABC transporter	3	3	152	252	5	5	270	98

554

555

556

Parsed Citations

Abida H, Dolch L-J, Meï C, Villanova V, Conte M, Block MA, Finazzi G, Bastien O, Tirichine L, Bowler C, Rébeillé F, Petroutsos D, Jouhet J, Maréchal E (2015) Membrane glycerolipid remodeling triggered by nitrogen and phosphorus starvation in *Phaeodactylum tricornutum*. *Plant Physiology* 167: 118-136

Pubmed: [Author and Title](#)

CrossRef: [Author and Title](#)

Google Scholar: [Author Only](#) [Title Only](#) [Author and Title](#)

Austin JR, Frost E, Vidi PA, Kessler F, Staehelin LA (2006) Plastoglobules are lipoprotein subcompartments of the chloroplast that are permanently coupled to thylakoid membranes and contain biosynthetic enzymes. *The Plant Cell* 18: 1693-1703

Pubmed: [Author and Title](#)

CrossRef: [Author and Title](#)

Google Scholar: [Author Only](#) [Title Only](#) [Author and Title](#)

Bligh E, Dyer W (1959) A rapid method of total lipid extraction and purification. *Can J Biochem Physiol* 37: 911 - 917

Pubmed: [Author and Title](#)

CrossRef: [Author and Title](#)

Google Scholar: [Author Only](#) [Title Only](#) [Author and Title](#)

Bonente G, Pippa S, Castellano S, Bassi R, Ballottari M (2012) Acclimation of *Chlamydomonas reinhardtii* to different growth irradiances. *Journal of Biological Chemistry* 287: 5833-5847

Pubmed: [Author and Title](#)

CrossRef: [Author and Title](#)

Google Scholar: [Author Only](#) [Title Only](#) [Author and Title](#)

Cagnon C, Mirabella B, Nguyen HM, Beyly-Adriano A, Bouvet S, Cuine S, Beisson F, Peltier G, Li-Beisson Y (2013) Development of a forward genetic screen to isolate oil mutants in the green microalga *Chlamydomonas reinhardtii*. *Biotechnology for Biofuels* 6: 178

Pubmed: [Author and Title](#)

CrossRef: [Author and Title](#)

Google Scholar: [Author Only](#) [Title Only](#) [Author and Title](#)

Chapman KD, Dyer JM, Mullen RT (2012) Biogenesis and functions of lipid droplets in plants: Thematic Review Series: Lipid droplet synthesis and metabolism: from Yeast to Man. *Journal of Lipid Research* 53: 215-226

Pubmed: [Author and Title](#)

CrossRef: [Author and Title](#)

Google Scholar: [Author Only](#) [Title Only](#) [Author and Title](#)

Chen H, Hu J, Qiao Y, Chen W, Rong J, Zhang Y, He C, Wang Q (2015) Ca²⁺-regulated cyclic electron flow supplies ATP for nitrogen starvation-induced lipid biosynthesis in green alga. *Scientific Reports* 5: 15117

Pubmed: [Author and Title](#)

CrossRef: [Author and Title](#)

Google Scholar: [Author Only](#) [Title Only](#) [Author and Title](#)

Dang K-V, Plet J, Tolleter D, Jokel M, Cuiñé S, Carrier P, Auroy P, Richaud P, Johnson X, Alric J, Allahverdiyeva Y, Peltier G (2014) Combined increases in mitochondrial cooperation and oxygen photoreduction compensate for deficiency in cyclic electron flow in *Chlamydomonas reinhardtii*. *The Plant Cell* 26: 3036-3050

Pubmed: [Author and Title](#)

CrossRef: [Author and Title](#)

Google Scholar: [Author Only](#) [Title Only](#) [Author and Title](#)

Dupieris V, Masselon C, Court M, Kieffer-Jaquinod S, Bruley C (2009) A toolbox for validation of mass spectrometry peptides identification and generation of database: IRMa. *Bioinformatics* 25: 1980-1981

Pubmed: [Author and Title](#)

CrossRef: [Author and Title](#)

Google Scholar: [Author Only](#) [Title Only](#) [Author and Title](#)

Erickson E, Wakao S, Niyogi KK (2015) Light stress and photoprotection in *Chlamydomonas reinhardtii*. *The Plant Journal* 82: 449-465

Pubmed: [Author and Title](#)

CrossRef: [Author and Title](#)

Google Scholar: [Author Only](#) [Title Only](#) [Author and Title](#)

Fan J, Yan C, Andre C, Shanklin J, Schwender J, Xu C (2012) Oil accumulation is controlled by carbon precursor supply for fatty acid synthesis in *Chlamydomonas reinhardtii*. *Plant and Cell Physiology* 53: 1380-1390

Pubmed: [Author and Title](#)

CrossRef: [Author and Title](#)

Google Scholar: [Author Only](#) [Title Only](#) [Author and Title](#)

Fan JL, Andre C, Xu CC (2011) A chloroplast pathway for the de novo biosynthesis of triacylglycerol in *Chlamydomonas reinhardtii*. *Fbs Letters* 585: 1985-1991

Pubmed: [Author and Title](#)

CrossRef: [Author and Title](#)

Google Scholar: [Author Only](#) [Title Only](#) [Author and Title](#)

Farese Jr RV, Walther TC (2009) Lipid droplets finally get a little R-E-S-P-E-C-T. *Cell* 139: 855-860

Pubmed: [Author and Title](#)

CrossRef: [Author and Title](#)

Google Scholar: [Author Only](#) [Title Only](#) [Author and Title](#)

Fischer BB, Wiesendanger M, Eggen RIL (2006) Growth condition-dependent sensitivity, photodamage and stress response of *Chlamydomonas reinhardtii* exposed to high light conditions. *Plant and Cell Physiology* 47: 1135-1145

Pubmed: [Author and Title](#)

CrossRef: [Author and Title](#)

Google Scholar: [Author Only](#) [Title Only](#) [Author and Title](#)

Forster B, Mathesius U, Pogson BJ (2006) Comparative proteomics of high light stress in the model alga *Chlamydomonas reinhardtii*. *Proteomics* 6: 4309-4320

Pubmed: [Author and Title](#)

CrossRef: [Author and Title](#)

Google Scholar: [Author Only](#) [Title Only](#) [Author and Title](#)

Goodman JM (2008) The gregarious lipid droplet. *Journal of Biological Chemistry* 283: 28005-28009

Pubmed: [Author and Title](#)

CrossRef: [Author and Title](#)

Google Scholar: [Author Only](#) [Title Only](#) [Author and Title](#)

Goodson C, Roth R, Wang ZT, Goodenough U (2011) Structural correlates of cytoplasmic and chloroplast lipid body synthesis in *Chlamydomonas reinhardtii* and stimulation of lipid body production with acetate boost. *Eukaryotic Cell* 10: 1592-1606

Pubmed: [Author and Title](#)

CrossRef: [Author and Title](#)

Google Scholar: [Author Only](#) [Title Only](#) [Author and Title](#)

Goold H, Beisson F, Peltier G, Li-Beisson Y (2015) Microalgal lipid droplets: composition, diversity, biogenesis and functions. *Plant Cell Reports* 34: 545-55

Pubmed: [Author and Title](#)

CrossRef: [Author and Title](#)

Google Scholar: [Author Only](#) [Title Only](#) [Author and Title](#)

Harris E (2001) *Chlamydomonas* as a model organism. *Annu Review Plant Physiol Plant Mol Biol* 52: 363 - 406

Pubmed: [Author and Title](#)

CrossRef: [Author and Title](#)

Google Scholar: [Author Only](#) [Title Only](#) [Author and Title](#)

He QN, Yang HJ, Wu L, Hu CX (2015) Effect of light intensity on physiological changes, carbon allocation and neutral lipid accumulation in oleaginous microalgae. *Bioresource Technology* 191: 219-228

Pubmed: [Author and Title](#)

CrossRef: [Author and Title](#)

Google Scholar: [Author Only](#) [Title Only](#) [Author and Title](#)

Hu Q, Sommerfeld M, Jarvis E, Ghirardi M, Posewitz M, Seibert M, Darzins A (2008) Microalgal triacylglycerols as feedstocks for biofuel production: perspectives and advances. *The Plant Journal* 54: 621-639

Pubmed: [Author and Title](#)

CrossRef: [Author and Title](#)

Google Scholar: [Author Only](#) [Title Only](#) [Author and Title](#)

Huang AHC (1992) Oil bodies and oleosins in seeds. *Annual Review of Plant Physiology and Plant Molecular Biology* 43: 177-200

Pubmed: [Author and Title](#)

CrossRef: [Author and Title](#)

Google Scholar: [Author Only](#) [Title Only](#) [Author and Title](#)

Huang AHC (1996) Oleosins and oil bodies in seeds and other organs. *Plant Physiology* 110: 1055-1061

Pubmed: [Author and Title](#)

CrossRef: [Author and Title](#)

Google Scholar: [Author Only](#) [Title Only](#) [Author and Title](#)

Jolivet P, Acevedo F, Boulard C, d'Andréa S, Faure J-D, Kohli A, Nesi N, Valot B, Chardot T (2013) Crop seed oil bodies: From challenges in protein identification to an emerging picture of the oil body proteome. *Proteomics* 13: 1836-1849

Pubmed: [Author and Title](#)

CrossRef: [Author and Title](#)

Google Scholar: [Author Only](#) [Title Only](#) [Author and Title](#)

Kandilian R, Pruvost J, Legrand J, Pilon L (2014) Influence of light absorption rate by *Nannochloropsis oculata* on triglyceride production during nitrogen starvation. *Bioresource Technology* 163: 308-319

Pubmed: [Author and Title](#)

CrossRef: [Author and Title](#)

Google Scholar: [Author Only](#) [Title Only](#) [Author and Title](#)

Kato N, Dong T, Bailey M, Lum T, Ingram D (2013) Triacylglycerol mobilization is suppressed by brefeldin A in *Chlamydomonas reinhardtii*. *Plant and Cell Physiology* 54: 1585-1599

Pubmed: [Author and Title](#)

CrossRef: [Author and Title](#)

Google Scholar: [Author Only](#) [Title Only](#) [Author and Title](#)

Kessler F, Vidi PA (2007) Plastoglobule lipid bodies: Their functions in chloroplasts and their potential for applications. In A Fiechter, C Sautter, eds, *Green Gene Technology: Research in an Area of Social Conflict*, Vol 107, pp 153-172

Pubmed: [Author and Title](#)

CrossRef: [Author and Title](#)

Google Scholar: [Author Only](#) [Title Only](#) [Author and Title](#)

Khotimchenko SV, Yakovleva IM (2005) Lipid composition of the red alga *Tichocarpus crinitus* exposed to different levels of photon irradiance. *Phytochemistry* 66: 73-79

Pubmed: [Author and Title](#)

CrossRef: [Author and Title](#)

Google Scholar: [Author Only](#) [Title Only](#) [Author and Title](#)

Khozin-Goldberg I, Cohen Z (2011) Unraveling algal lipid metabolism: Recent advances in gene identification. *Biochimie* 93: 91-100

Pubmed: [Author and Title](#)

CrossRef: [Author and Title](#)

Google Scholar: [Author Only](#) [Title Only](#) [Author and Title](#)

Kim H, Jang S, Kim S, Yamaoka Y, Hong D, Song W, Nishida I, Li-Beisson Y, Lee Y (2015) The small molecule fenpropimorph rapidly converts chloroplast membrane lipids to triacylglycerols in *Chlamydomonas reinhardtii*. *Frontiers in Microbiology* 6: 54

Pubmed: [Author and Title](#)

CrossRef: [Author and Title](#)

Google Scholar: [Author Only](#) [Title Only](#) [Author and Title](#)

Kim S, Kim H, Ko D, Yamaoka Y, Otsuru M, Kawai-Yamada M, Ishikawa T, Oh H-M, Nishida I, Li-Beisson Y, Lee Y (2013) Rapid induction of lipid droplets in *Chlamydomonas reinhardtii* and *Chlorella vulgaris* by brefeldin A. *PLoS ONE* 8: e81978

Pubmed: [Author and Title](#)

CrossRef: [Author and Title](#)

Google Scholar: [Author Only](#) [Title Only](#) [Author and Title](#)

Klein U, Betz A (1978) Fermentative metabolism of hydrogen-evolving *Chlamydomonas moewusii*. *Plant Physiology* 61: 953-956

Pubmed: [Author and Title](#)

CrossRef: [Author and Title](#)

Google Scholar: [Author Only](#) [Title Only](#) [Author and Title](#)

Klok AJ, Martens DE, Wijffels RH, Lamers PP (2013) Simultaneous growth and neutral lipid accumulation in microalgae. *Bioresource Technology* 134: 233-243

Pubmed: [Author and Title](#)

CrossRef: [Author and Title](#)

Google Scholar: [Author Only](#) [Title Only](#) [Author and Title](#)

Légeret B, Schulz-Raffelt M, Nguyen HM, Auroy P, Beisson F, Peltier G, Blanc G, Li-Beisson Y (2016) Lipidomic and transcriptomic analyses of *Chlamydomonas reinhardtii* under heat stress unveil a direct route for the conversion of membrane lipids into storage lipids. *Plant, Cell & Environment*: 39:834 -847

Pubmed: [Author and Title](#)

CrossRef: [Author and Title](#)

Google Scholar: [Author Only](#) [Title Only](#) [Author and Title](#)

Li-Beisson Y, Beisson F, Riekhof W (2015) Metabolism of acyl-lipids in *Chlamydomonas reinhardtii*. *The Plant Journal* 82: 504-522

Pubmed: [Author and Title](#)

CrossRef: [Author and Title](#)

Google Scholar: [Author Only](#) [Title Only](#) [Author and Title](#)

Li YH, Beisson F, Pollard M, Ohlrogge J (2006) Oil content of *Arabidopsis* seeds: The influence of seed anatomy, light and plant-to-plant variation. *Phytochemistry* 67: 904-915

Pubmed: [Author and Title](#)

CrossRef: [Author and Title](#)

Google Scholar: [Author Only](#) [Title Only](#) [Author and Title](#)

Liu B, Benning C (2013) Lipid metabolism in microalgae distinguishes itself. *Current Opinion in Biotechnology* 24: 300-309

Pubmed: [Author and Title](#)

CrossRef: [Author and Title](#)

Google Scholar: [Author Only](#) [Title Only](#) [Author and Title](#)

Ma X, Liu J, Liu B, Chen T, Yang B, Chen F (2016) Physiological and biochemical changes reveal stress-associated photosynthetic carbon partitioning into triacylglycerol in the oleaginous marine alga *Nannochloropsis oculata*. *Algal Research* 16: 28-35

Pubmed: [Author and Title](#)

CrossRef: [Author and Title](#)

Google Scholar: [Author Only](#) [Title Only](#) [Author and Title](#)

Martinis J, Glauser G, Valimareanu S, Kessler F (2013) A chloroplast ABC1-like kinase regulates vitamin E metabolism in *Arabidopsis*. *Plant Physiology* 162: 652-662

Pubmed: [Author and Title](#)

CrossRef: [Author and Title](#)

Google Scholar: [Author Only](#) [Title Only](#) [Author and Title](#)

Merchant SS, Kropat J, Liu B, Shaw J, Warakanont J (2012) TAG, You're it! *Chlamydomonas* as a reference organism for understanding algal triacylglycerol accumulation. *Current Opinion in Biotechnology* 23: 352-363

Pubmed: [Author and Title](#)

CrossRef: [Author and Title](#)

Google Scholar: [Author Only](#) [Title Only](#) [Author and Title](#)

Mettler T, Mühlhaus T, Hemme D, Schöttler M-A, Rupprecht J, Idoine A, Veyel D, Pal SK, Yaneva-Roder L, Winck FV, Sommer F, Vosloh D, Seiwert B, Erban A, Burgos A, Arvidsson S, Schönfelder S, Arnold A, Günther M, Krause U, Lohse M, Kopka J, Nikoloski Z, Mueller-Roeber B, Willmitzer L, Bock R, Schroda M, Stitt M (2014) Systems analysis of the response of photosynthesis, metabolism, and growth to an increase in irradiance in the photosynthetic model organism *Chlamydomonas reinhardtii*. *The Plant Cell* 26: 2310-2350

Pubmed: [Author and Title](#)
CrossRef: [Author and Title](#)
Google Scholar: [Author Only](#) [Title Only](#) [Author and Title](#)

Moellering ER, Benning C (2010) RNA interference silencing of a major lipid droplet protein affects lipid droplet size in *Chlamydomonas reinhardtii*. Eukaryotic Cell 9: 97-106

Pubmed: [Author and Title](#)
CrossRef: [Author and Title](#)
Google Scholar: [Author Only](#) [Title Only](#) [Author and Title](#)

Nguyen HM, Baudet M, Cuiné S, Adriano J-M, Barthe D, Billon E, Bruley C, Beisson F, Peltier G, Ferro M, Li-Beisson Y (2011) Proteomic profiling of oil bodies isolated from the unicellular green microalga *Chlamydomonas reinhardtii*: With focus on proteins involved in lipid metabolism. Proteomics 11: 4266-4273

Pubmed: [Author and Title](#)
CrossRef: [Author and Title](#)
Google Scholar: [Author Only](#) [Title Only](#) [Author and Title](#)

Nguyen HM, Cuiné S, Beyly-Adriano A, Légeret B, Billon E, Auroy P, Beisson F, Peltier G, Li-Beisson Y (2013) The green microalga *Chlamydomonas reinhardtii* has a single Δ^3 fatty acid desaturase that localizes to the chloroplast and impacts both plastidic and extraplastidic membrane lipids. Plant Physiology 163: 914-928

Pubmed: [Author and Title](#)
CrossRef: [Author and Title](#)
Google Scholar: [Author Only](#) [Title Only](#) [Author and Title](#)

Pal D, Khozin-Goldberg I, Cohen Z, Boussiba S (2011) The effect of light, salinity, and nitrogen availability on lipid production by *Nannochloropsis* sp. Applied Microbiology and Biotechnology 90: 1429-1441

Pubmed: [Author and Title](#)
CrossRef: [Author and Title](#)
Google Scholar: [Author Only](#) [Title Only](#) [Author and Title](#)

Peers G, Truong TB, Ostendorf E, Busch A, Elrad D, Grossman AR, Hippler M, Niyogi KK (2009) An ancient light-harvesting protein is critical for the regulation of algal photosynthesis. Nature 462: 518-521

Pubmed: [Author and Title](#)
CrossRef: [Author and Title](#)
Google Scholar: [Author Only](#) [Title Only](#) [Author and Title](#)

Rosenberg JN, Oyley GA, Wilkinson L, Betenbaugh MJ (2008) A green light for engineered algae: redirecting metabolism to fuel a biotechnology revolution. Current Opinion in Biotechnology 19: 430-436

Pubmed: [Author and Title](#)
CrossRef: [Author and Title](#)
Google Scholar: [Author Only](#) [Title Only](#) [Author and Title](#)

Sambrook J, Russell DW (2001) Molecular cloning : a laboratory manual. Cold Spring Harbor, N.Y. : Cold Spring Harbor Laboratory, c2001.

Pubmed: [Author and Title](#)
CrossRef: [Author and Title](#)
Google Scholar: [Author Only](#) [Title Only](#) [Author and Title](#)

Sato R, Ito H, Tanaka A (2015) Chlorophyll b degradation by chlorophyll b reductase under high-light conditions. Photosynthesis Research 126: 249-259

Pubmed: [Author and Title](#)
CrossRef: [Author and Title](#)
Google Scholar: [Author Only](#) [Title Only](#) [Author and Title](#)

Scott SA, Davey MP, Dennis JS, Horst I, Howe CJ, Lea-Smith DJ, Smith AG (2010) Biodiesel from algae: challenges and prospects. Current Opinion in Biotechnology 21: 277-286

Pubmed: [Author and Title](#)
CrossRef: [Author and Title](#)
Google Scholar: [Author Only](#) [Title Only](#) [Author and Title](#)

Sheehan J, Dunahay, T., Benemann, J. and Roessler, P.G. (1998) A look back at the US Department of Energy's aquatic species program - biodiesel from algae. In. US Department of Energy's Office of Fuels Development, Golden, CO: National Renewable Energy Laboratory.

Pubmed: [Author and Title](#)
CrossRef: [Author and Title](#)
Google Scholar: [Author Only](#) [Title Only](#) [Author and Title](#)

Siaut M, Cuine S, Cagnon C, Fessler B, Nguyen M, Carrier P, Beyly A, Beisson F, Triantaphylides C, Li-Beisson Y, Peltier G (2011) Oil accumulation in the model green alga *Chlamydomonas reinhardtii*: characterization, variability between common laboratory strains and relationship with starch reserves. BMC Biotechnology 11: 7

Pubmed: [Author and Title](#)
CrossRef: [Author and Title](#)
Google Scholar: [Author Only](#) [Title Only](#) [Author and Title](#)

Tardif M, Atteia A, Specht M, Cogne G, Rolland N, Brugière S, Hippler M, Ferro M, Bruley C, Peltier G, Vallon O, Cournac L (2012) PredAlgo, a new subcellular localization prediction tool dedicated to green algae. Molecular Biology and Evolution 29: 3625-3639

Pubmed: [Author and Title](#)
CrossRef: [Author and Title](#)
Google Scholar: [Author Only](#) [Title Only](#) [Author and Title](#)

Tolletier D, Ghysels B, Alric J, Petroutsos D, Tolstygina I, Krawietz D, Happe T, Auroy P, Adriano JM, Beyly A, Cuine S, Plet J, Reiter IM, Genty B, Cournac L, Hippler M, Peltier G (2011) Control of hydrogen photoproduction by the proton gradient generated by cyclic electron flow in *Chlamydomonas reinhardtii*. *The Plant Cell* 23: 2619-2630

Pubmed: [Author and Title](#)

CrossRef: [Author and Title](#)

Google Scholar: [Author Only](#) [Title Only](#) [Author and Title](#)

Tsai C-H, Warakanont J, Takeuchi T, Sears BB, Moellering ER, Benning C (2014) The protein Compromised Hydrolysis of Triacylglycerols 7 (CHT7) acts as a repressor of cellular quiescence in *Chlamydomonas*. *Proceedings of the National Academy of Sciences* 111: 15833-15838

Pubmed: [Author and Title](#)

CrossRef: [Author and Title](#)

Google Scholar: [Author Only](#) [Title Only](#) [Author and Title](#)

Tsai C-H, Zienkiewicz K, Amstutz CL, Brink BG, Warakanont J, Roston R, Benning C (2015) Dynamics of protein and polar lipid recruitment during lipid droplet assembly in *Chlamydomonas reinhardtii*. *The Plant Journal* 83: 650-660

Pubmed: [Author and Title](#)

CrossRef: [Author and Title](#)

Google Scholar: [Author Only](#) [Title Only](#) [Author and Title](#)

Tzen JTC, Huang AHC (1992) Surface structure and properties of plant seed oil bodies. *Journal of Cell Biology* 117: 327-335

Pubmed: [Author and Title](#)

CrossRef: [Author and Title](#)

Google Scholar: [Author Only](#) [Title Only](#) [Author and Title](#)

Urzica EI, Vieler A, Hong-Hermesdorf A, Page MD, Casero D, Gallaher SD, Kropat J, Pellegrini M, Benning C, Merchant SS (2013) Remodeling of membrane lipids in iron-starved *Chlamydomonas*. *Journal of Biological Chemistry* 288: 30246-30258

Pubmed: [Author and Title](#)

CrossRef: [Author and Title](#)

Google Scholar: [Author Only](#) [Title Only](#) [Author and Title](#)

Wang ZT, Ullrich N, Joo S, Waffenschmidt S, Goodenough U (2009) Algal lipid bodies: stress induction, purification, and biochemical characterization in wild-type and starchless *Chlamydomonas reinhardtii*. *Eukaryot Cell* 8: 1856-1868

Pubmed: [Author and Title](#)

CrossRef: [Author and Title](#)

Google Scholar: [Author Only](#) [Title Only](#) [Author and Title](#)

Wijffels RH, Barbosa MJ (2010) An outlook on microalgal biofuels. *Science* 329: 796-799

Pubmed: [Author and Title](#)

CrossRef: [Author and Title](#)

Google Scholar: [Author Only](#) [Title Only](#) [Author and Title](#)

Zhekisheva M, Boussiba S, Khozin-Goldberg I, Zarka A, Cohen Z (2002) Accumulation of oleic acid in *Haematococcus pluvialis* (chlorophyceae) under nitrogen starvation or high light is correlated with that of astaxanthin esters. *Journal of Phycology* 38: 325-331

Pubmed: [Author and Title](#)

CrossRef: [Author and Title](#)

Google Scholar: [Author Only](#) [Title Only](#) [Author and Title](#)